



TRIANGULAR EXCHANGE DIAGRAM WITHIN THE FULL OFF-SHELL COULOMB T-MATRIX IN DEUTERON INDUCED REACTIONS

T. V. Nhan Hao*, N. Nhu Le, Pham Huong Thao

Center for Theoretical and Computational Physics, University of Education, Hue University,
34 Le Loi Street, Hue City, Vietnam

Abstract: The amplitude of the triangular diagrams in the three-body models of deuteron induced reactions with charged particles contains the off-shell two-body T -matrix describing the intermediate-state Coulomb scattering of charged subsystems. Up to now the latter has usually been replaced by the Coulomb potential due to the computational reason. In this paper, we first investigate theoretically and numerically the validity of the mentioned Coulomb-Born approximation. The results show the important contribution of the higher order of the latter approximation for the (d,p) reactions off heavy target.

1 Introduction

Treatment the long-range character of the Coulomb interaction in low-energy deuteron induced-reactions off heavy targets using the 3-body Faddeev formalism [1] is a challenging task. In principle, scattering of deuteron off a nuclear target (an inert core A) can be exactly described in the framework of the Faddeev integral equations written in the AGS form [2]. The latter equations are usually solved in momentum-space partial-wave basis where they become a system of integral equations with two continuous momenta variables. However, the Faddeev-AGS formalism is only designed for short-range potentials. In fact the long-range behavior of Coulomb interaction gives rise to severe singularities in the kernel of the integral equation that the latter may lack the compactness property known to exist in the case of purely short-range interactions. One way of dealing with this problem is to use the screening and renormalization method [3, 5] which has successfully described not only the 3-body but also 4-body nuclear systems [6-10]. Unfortunately, the technical difficulties arise in the renormalization procedure as the charge of the target increases making this approach is unreliable for targets with charge $Z \geq 28$ [11]. So after almost 50 years from the pioneer works of A. M. Veselova [4], the Coulomb potential remains a serious barrier for having an accurate description of low-energy nuclear reactions using the three-body Faddeev integral equations. New approach based on employing the non-screened Coulomb potential is derived [12]. Instead of the usual plane-wave basis, the AGS equations are cast in a momentum-space Coulomb distorted partial-wave representation. Applying two potential formulas the AGS equations are converted to the form in which the matrix elements are sandwiched by the Coulomb distorted waves in the initial and final states. The obtained Faddeev-

* Corresponding: tran.viet.nhan.hao@gmail.com

AGS equations couple all the neutron transfer, proton transfer, in(elastic) scattering, and triangular exchange diagrams (see Fig. 1). The channel Coulomb potentials [sub-diagram (e)] are subtracted from the in(elastic) diagram to remove the strongest singularity of the elastic scattering triangular diagram with Coulomb four-ray vertex which leads to a noncompact singularity of the Faddeev-AGS equations [3, 5, 11]. These generalized Faddeev-AGS equations provide the most advanced and complete description of the deuteron induced reactions. Despite the core formalism having been developed, in order to make it practical an important additional analytical and computational work is required.

In this paper, we propose a new method to approximately take into account the triangular exchange diagrams instead of directly calculating it. Through this investigation we also show for the first time the role of the full off-shell Coulomb T-matrix in describing the intermediate-state Coulomb scattering of proton and target. In the previous works [13-15], the Coulomb T-matrix is usually replaced by the corresponding Coulomb potential. This approximation considerably reduces the analytical and numerical efforts due to the treatment of the full off-shell Coulomb T matrix. As has been shown in Refs. [16, 17], the Coulomb-Born approximation is accurate to a few percent for all energies and scattering angles for the d(p,d)p reaction. *A priori*, the increase of the charge of the nuclear targets gives rise to the uncertainties of the Coulomb-Born approximation. To the best of our knowledge the validity of the latter approximation is still an open question in the region of medium and heavy targets.

2 Theoretical Formalism

We consider the system consisting of two nucleons (1 proton and 1 neutron) and a nucleus consisting of A nucleons (no core excitation) to the three-body system. Denote the masses of the

three particles by m_γ , $\gamma = 1, 2, 3$, and the reduced mass of pair (α, β) is $\mu_\gamma = \frac{m_\alpha m_\beta}{m_{\alpha\beta}}$,

$M_\alpha = \frac{m_\alpha m_{\beta\gamma}}{m_\alpha + m_\beta + m_\gamma}$, $M_\beta = \frac{m_\beta m_{\alpha\gamma}}{m_\alpha + m_\beta + m_\gamma}$, and $\mathcal{M} = m_\alpha + m_\beta + m_\gamma$. The sub-figure (d) of the

Fig. 1 shows the exchange process from the initial channel $\alpha + (\beta\gamma)$ to the final channel $\beta + (\alpha\gamma)$ where particle α having a center-of-mass (c.m.) momentum p_α impinges on the bound state of particles β and γ and in the final state particles γ and α are bound in a state and particle β is free with a c.m. momentum p'_β . This triangular exchange diagram is nothing else the neutron transfer diagram taking into account the Coulomb scattering between the proton and the target. First, we analytically demonstrate that the inclusion of a four-ray vertex corresponding to the off-energy shell Coulomb scattering in the triangular exchange diagram will affect neither the position nor the character of the proper singularity in $\cos(\theta)$ (θ is the scattering angle in c.m.) of

the neutron transfer diagram (pole diagram). The magnitude of the triangular exchange diagram ($\alpha \neq \beta \neq \gamma \neq \alpha$) is given by (see also Ref. [18-20])

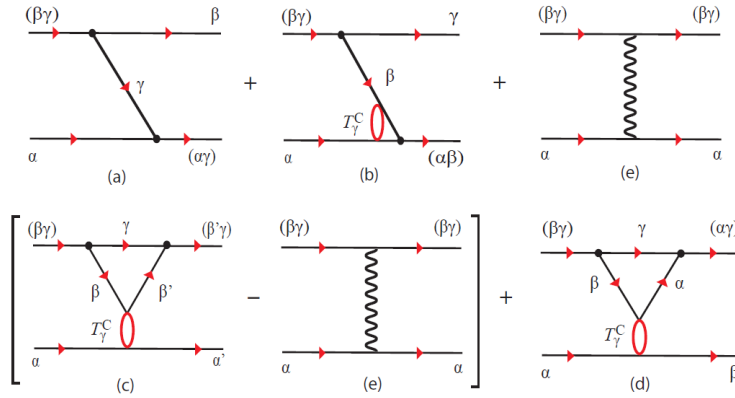


Fig. 1. Diagrammatical representation of the effective potential of the Faddeev-AGS equations describing the deuteron induced reactions. It includes: the neutron transfer diagram [sub-figure (a)], the proton transfer diagram [sub-figure (b)], in(elastic) scattering [sub-figure (c)], and the triangular exchange amplitude [sub-figure (d)]. The strongest singularity of the elastic scattering triangular diagram is compensated by the subtracted channel Coulomb potential [sub-diagram (e)]. Bubble shows the full off-shell Coulomb scattering amplitude of proton and target

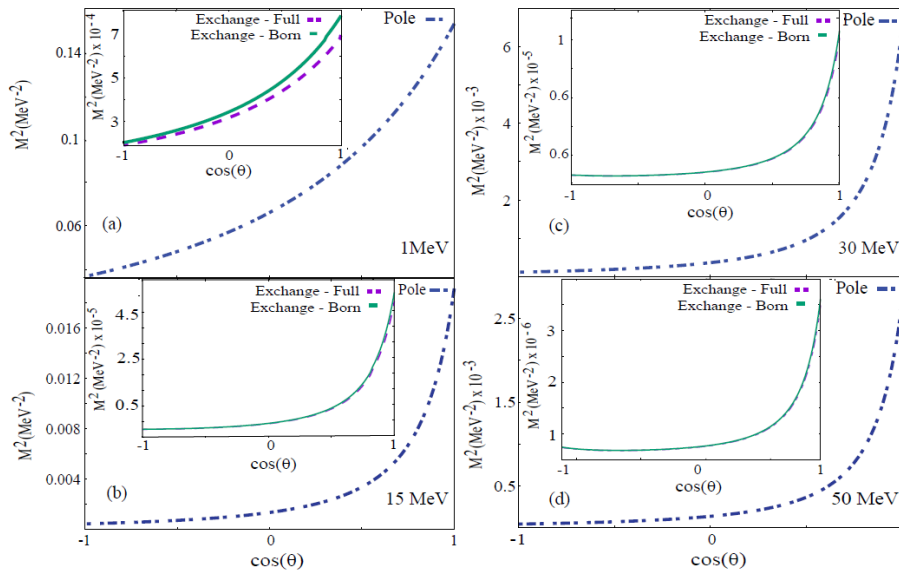


Fig. 2. The dot-dashed lines show the magnitude of the neutron transfer diagram whereas the solid (dashed) lines present the triangular exchange amplitude with (without) Coulomb-Born approximation for the $d(p,d)p$ reactions at 1, 15, 30, and 50 MeV

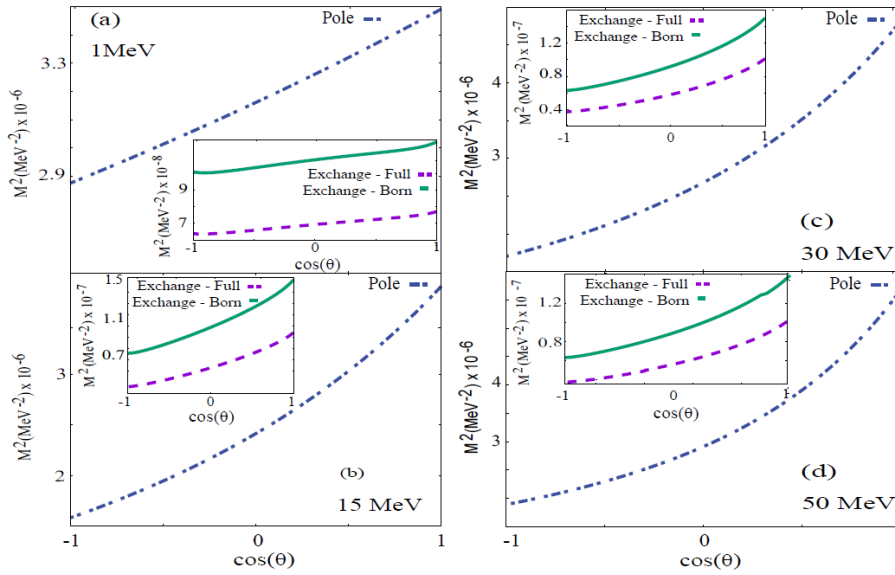


Fig. 3. The dot-dashed lines show the magnitude of the neutron transfer diagram whereas the solid (dashed) lines present the triangular exchange amplitude with (without) Coulomb-Born approximation for the $^{48}\text{Ca}(p,d)^{49}\text{Ca}$ reactions at 1, 15, 30, and 50 MeV

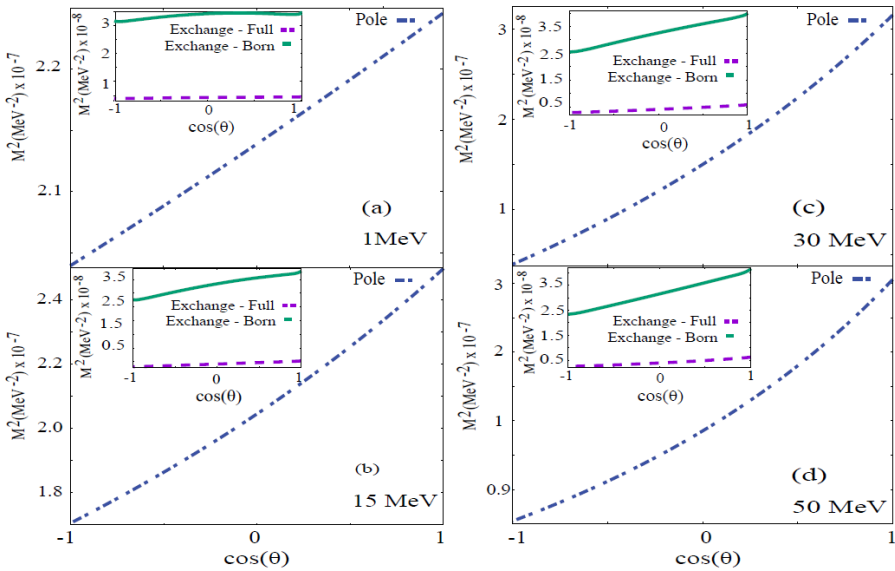


Fig. 4. The dot-dashed lines show the magnitude of the neutron transfer diagram whereas the solid (dashed) lines present the triangular exchange amplitude with (without) Coulomb-Born approximation for the $^{208}\text{Pb}(p,d)^{209}\text{Pb}$ reactions at 1, 15, 30, and 50 MeV

$$M_{\text{Full}}^{(d)}(p'_\beta, p_\alpha; z) = 4\mu_\beta \mu_\alpha \int \frac{dp_\gamma}{(2\pi)^3} \frac{1}{\hat{k}_\beta^2 - (p_\gamma + \frac{m_\gamma}{m_{\alpha\gamma}} p'_\beta)^2} T_\gamma^C(k'_\gamma, k_\gamma; \hat{z}_\gamma) \frac{1}{\hat{k}_\alpha^2 - (-p_\gamma + \frac{m_\gamma}{m_{\beta\gamma}} p_\alpha)^2}, \quad (1)$$

where $\hat{k}_\alpha^2 = 2\mu_\alpha \hat{z}_\alpha$ and $\hat{z}_\alpha = (z - \frac{p_\alpha^2}{2M_\alpha})$; $\hat{k}_\beta^2 = 2\mu_\beta \hat{z}_\beta$ and $\hat{z}_\beta = (z - \frac{p_\beta'^2}{2M_\beta})$; p_γ is the momentum of the transfer particle. The standard expression for the off-shell Coulomb scattering amplitude is [18-20].

$$T_\gamma^C(k'_\gamma, k_\gamma; \hat{z}_\gamma) = 4\pi Z_\alpha Z_\beta e^2 \left[\frac{1}{(k_\gamma - k'_\gamma)^2} - i\eta_\gamma I(k'_\gamma, k_\gamma; \hat{z}_\gamma) \right], \quad (2)$$

$$I(k'_\gamma, k_\gamma; \hat{z}_\gamma) = \lim_{\varepsilon \rightarrow 0} \int_0^1 dx x^{m_\gamma} \frac{1}{x(k_\gamma - k'_\gamma)^2 - \frac{\mu_\gamma}{2\hat{z}_\gamma} [\hat{z}_\gamma + i\varepsilon - k_\gamma^2 / (2\mu_\gamma)] [\hat{z}_\gamma + i\varepsilon - k_\gamma'^2 / (2\mu_\gamma)] (1-x)^2}, \quad (3)$$

where k_γ and k'_γ are the relative off-shell momenta of charged particles α and β before and after scattering moving with the relative kinetic energy \hat{z}_γ , $\eta_\gamma = Z_\alpha Z_\beta e^2 \mu_\gamma / k_\gamma$ and $k_\gamma = \sqrt{2\mu_\gamma \hat{z}_\gamma}$.

The closest to the physical region and the strongest singularity of the triangular exchange diagram is the one generated by the coincidence of the singularities of the propagators $\hat{k}_\alpha^2 - (-p_\gamma + \frac{m_\gamma}{m_{\beta\gamma}} p_\alpha)^2 = 0$ and $\hat{k}_\beta^2 - (p_\gamma + \frac{m_\gamma}{m_{\alpha\gamma}} p'_\beta)^2 = 0$ and the forward singularity of the off-shell Coulomb singularity $\Delta_\gamma = (k_\gamma - k'_\gamma)^2 = 0$ of the Coulomb scattering amplitude. To show how these singularity of the triangular exchange diagram appears and to simplify consideration we replace the off-shell Coulomb scattering amplitude $T_\gamma^C(k'_\gamma, k_\gamma; \hat{z}_\gamma)$ of particles α and β by the Coulomb-Born amplitude, which is the Fourier transform of the Coulomb potential $4\pi / \Delta_\gamma^2$. Then the amplitude of triangular exchange diagram simplifies to

$$M_{\text{Born}}^{(d)}(p'_\beta, p_\alpha) = 16\mu_\alpha \mu_\beta \pi Z_\beta Z_\alpha e^2 \int \frac{d\Delta_\gamma}{(2\pi)^3} \frac{1}{\hat{k}_\beta^2 - (\Delta_\gamma - k'_\beta)^2} \frac{1}{\Delta_\gamma^2} \frac{1}{\hat{k}_\alpha^2 - (\Delta_\gamma - k_\alpha)^2}, \quad (4)$$

where we used the substitution $p_\gamma = \Delta_\gamma - p_\alpha - p'_\beta$. Also $k_\alpha = p'_\beta + (m_\beta / m_{\beta\gamma}) p_\alpha$ is the relative momentum of particles β and γ in the three-ray vertex $(\beta\gamma) \rightarrow \beta + \gamma$. Similarly

$\mathbf{k}'_\beta = \mathbf{p}_\alpha + (m_\alpha / m_{\alpha\gamma})\mathbf{p}'_\beta$ is the relative momentum of particles α and γ in the three-ray vertex $(\alpha\gamma) \rightarrow \alpha + \gamma$ of the same diagram. Now we rewrite

$$\hat{k}_\alpha^2 - (\Delta_\gamma - \mathbf{k}_\alpha)^2 = \sigma_\alpha + 2\Delta_\gamma \cdot \mathbf{k}_\alpha - \Delta_\gamma^2 = \sigma_\alpha [1 + 2t \cdot \mathbf{k}_\alpha - \sigma_\alpha t^2], \quad (5)$$

where we introduced $\sigma_\alpha = \hat{k}_\alpha^2 - \mathbf{k}_\alpha^2$ and used the substitution

$$\Delta_\gamma = \sigma_\alpha t. \quad (6)$$

Similarly

$$\hat{k}_\beta^2 - (\Delta_\gamma - \mathbf{k}'_\beta)^2 = \sigma_\alpha \left[\frac{\mu_\beta}{\mu_\alpha} + 2t \cdot \mathbf{k}'_\beta - \sigma_\alpha t^2 \right]. \quad (7)$$

Here we took into account that from the energy-momentum conservation in both three-ray vertices of the diagram (b) in Fig. 1 follows

$$\sigma_\beta = \frac{\mu_\beta}{\mu_\alpha} \sigma_\alpha. \quad (8)$$

Because we consider the singularity of the triangular exchange diagram generated by the coincidence of zeroes of three denominators (pinch-point singularity) in Eq. (4), we use the substitution (6) obtaining in the leading order

$$M_{\text{Born}}^{(d)}(\mathbf{p}'_\beta, \mathbf{p}_\alpha)^{\sigma_\alpha \rightarrow 0} \sim \frac{1}{\sigma_\alpha} \int \frac{dt}{(2\pi)^3} \frac{1}{\frac{\mu_\beta}{\mu_\alpha} + 2t \cdot \mathbf{k}'_\beta} \frac{1}{t^2} \frac{1}{1 + 2t \cdot \mathbf{k}_\alpha} = \frac{1}{\sigma_\alpha} \int \frac{dt}{(2\pi)^3} \frac{1}{D_1} \frac{1}{t^2} \frac{1}{D_2}. \quad (9)$$

Thus we have shown that the strongest singularity of the amplitude of the triangular exchange diagram is a pole singularity at

$$\sigma_\alpha = 0. \quad (10)$$

The same singularity has the pole diagram in sub-figure (a) in Fig. 1. Moreover

$$M^{(a)}(\mathbf{p}'_\beta, \mathbf{p}_\alpha) \sim \frac{1}{\sigma_\alpha} \quad (11)$$

in Eq. (9) is the amplitude of the pole diagram. We can conclude from the simple consideration presented here that near the singularity (10) the amplitude of the triangular exchange diagram behaves as renormalized amplitude of the pole diagram in sub-figure (a) of Fig. 1:

$$M_{\text{Born}}^{(d)}(\mathbf{p}'_{\beta}, \mathbf{p}_{\alpha}) \stackrel{\sigma_{\alpha} \rightarrow 0}{=} D_{\beta\alpha} M^{(a)}(\mathbf{p}'_{\beta}, \mathbf{p}_{\alpha}) + M_{\text{reg}}^{(b)}(\mathbf{p}'_{\beta}, \mathbf{p}_{\alpha}), \quad (12)$$

where $D_{\beta\alpha}$ is the renormalization factor determining the strength of the pole singularity. The additional term $M_{\text{reg}}^{(b)}(\mathbf{p}'_{\beta}, \mathbf{p}_{\alpha})$ is regular at $\sigma_{\alpha} = 0$. A general expression for the renormalization factor for the triangular exchange diagram containing the full T_{γ}^C Coulomb scattering amplitude rather than the Coulomb-Born amplitude was obtained in [21-23]. The renormalization factor, which determines the strength of the pole singularity of the triangular exchange diagram, is

$$D_{\beta\alpha} = -1 + \left(\frac{\sqrt{m_{\beta\gamma} m_{\alpha} \varepsilon_{\beta\gamma}} + \sqrt{m_{\alpha\gamma} m_{\beta} \varepsilon_{\alpha\gamma}} + i\sqrt{m_{\gamma} m_{\beta\alpha} E_{\beta\alpha}}}{\sqrt{m_{\beta\gamma} m_{\alpha} \varepsilon_{\beta\gamma}} + \sqrt{m_{\alpha\gamma} m_{\beta} \varepsilon_{\alpha\gamma}} - i\sqrt{m_{\gamma} m_{\beta\alpha} E_{\beta\alpha}}} \right)^{i\eta_{\beta\alpha}}, \quad (13)$$

$$E_{\beta\alpha} = \frac{\mathcal{M}}{m_{\beta\alpha}}(z + i0) + \frac{m_{\alpha\gamma} \varepsilon_{\alpha\gamma}}{m_{\beta\alpha}} + \frac{m_{\beta\gamma} \varepsilon_{\beta\gamma}}{m_{\beta\alpha}}, \quad (14)$$

$$\eta_{\beta\alpha} = \frac{Z_{\beta} Z_{\alpha} e^2 \mu_{\beta\alpha}}{\sqrt{2\mu_{\beta\alpha} E_{\beta\alpha}}}. \quad (15)$$

3 Conclusions

The analytical results have been demonstrated by the numerical calculations presented in Figs. 2, 3, and 4. The magnitude of the pole and triangular exchange diagrams have been calculated for ${}^2\text{H}$, ${}^{48}\text{Ca}$ and ${}^{208}\text{Pb}$ targets at different energies below 50 MeV. The proper singularity of triangular exchange diagram (arising as result of simultaneous vanishing of D_1 and D_2 in the denominator of Eq. (9) appears for d(p,d)p reaction at energy higher than 30 MeV, and this singularity located farther from the physical domain than the pole singularity. Based on the obtained results, we can considerably simplify the calculations of the effective potentials of Faddeev-AGS equations by combining the neutron transfer pole amplitudes with the Coulomb exchange triangular diagram amplitudes taking into account the fact that near the pole the exchange triangular diagram has also a pole singularity.

To investigate the validity of the Coulomb-Born approximation, it is useful to define the ratio of the full off-shell Coulomb T-matrix to the Coulomb potential scattering magnitude $R = |M_{\text{Full}}^{(d)} / M_{\text{Born}}^{(d)}|^2$ which measures the quality of the Coulomb-Born approximation. Fig. 5 shows the quantity R for the (d, p) reactions off ${}^2\text{H}$, ${}^{48}\text{Ca}$ and ${}^{208}\text{Pb}$ targets at different energies below 50 MeV. In the light-target region, the Coulomb-Born approximation works very well even at very low energy around 1 MeV. The obtained results show that the Coulomb-Born

approximation is more accurate at small scattering angles less than 80 degree. It fails rather dramatically in the medium and completely collapses in heavy regions at any energies below 50 MeV. We could conclude that the full off-shell Coulomb T matrix must be taken into account for the (d,p) reactions off the medium and heavy targets.

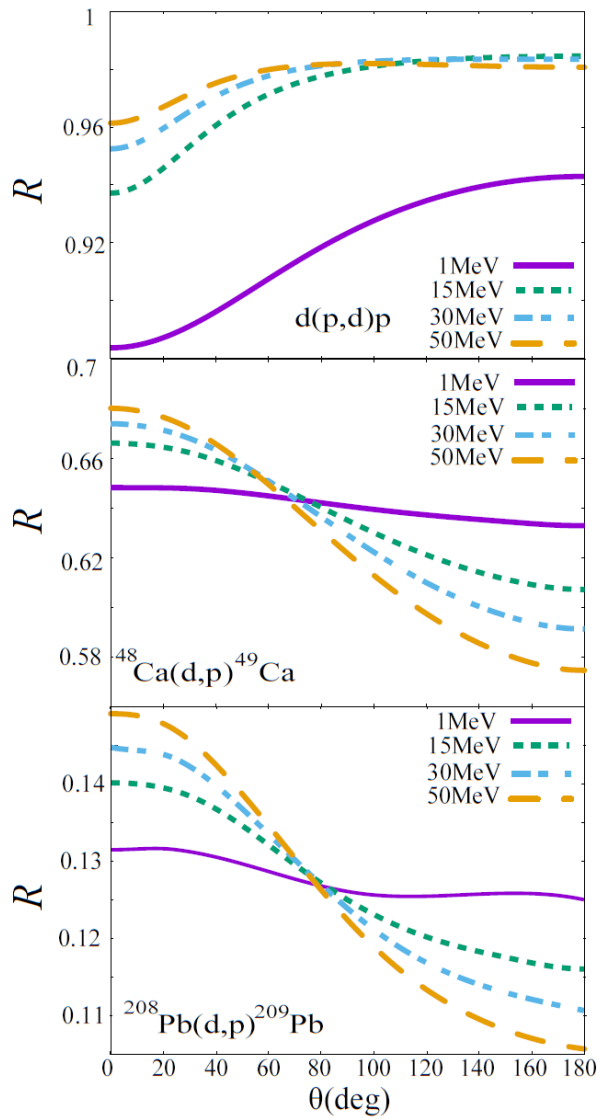


Fig. 5. The ratio of the full off-shell Coulomb T-matrix to the Coulomb potential scattering magnitudes in function of mass of the target at 1, 15, 30, and 50 MeV

This work will serve as basis for future (d,p) reactions code based on the Faddeev-AGS equations. This code allows us to extract the information from (n, γ) reactions off the targets from very light to heavy region in the nuclear chart.

Acknowledgments

This work is funded by the National Foundation for Science and Technology Development (NAFOSTED) of Vietnam through Grant No. 103.04-2017.69. One of the authors (N. Nhu Le) acknowledges the support by Hue University Grant No. DHH 2017-03-100.

References

1. L. D. Faddeev (1961), "Scattering theory for a three-particle system", *Soviet Phys.-JETP* 12, pp. 1014.
2. E. O. Alt, P. Grassberger, and W. Sandhas (1967), "Reduction of the three-particle collision problem to multi-channel two-particle Lippmann-Schwinger equations", *Nucl. Phys. B2*, pp 167.
3. E. O. Alt, W. Sandhas, and H. Ziegelmann (1978), "Coulomb effects in three-body reactions with two charged particles", *Phys. Rev. C* 17, pp 1981.
4. A. M. Veselova (1970), "Separation of two-particle Coulomb singularities in a system of three charged particles", *Theor. Math. Phys.* 3, pp 542.
5. E. O. Alt and W. Sandhas (1980), "Scattering amplitudes and integral equations for the collision of two charged composite particles", *Phys. Rev. C* 21, pp 1733.
6. A. Deltuva and A. C. Fonseca (2009), "Three-body Faddeev-Alt-Grassberger-Sandhas approach to direct nuclear reactions", *Phys. Rev. C* 79, 014606.
7. A. Deltuva (2009), "Three-body direct nuclear reactions: Nonlocal optical potential", *Phys. Rev. C* 79, 021602.
8. A. Deltuva (2009), "Deuteron stripping and pickup involving the halo nuclei ^{11}Be and ^{15}C ", *Phys. Rev. C* 79, 054603.
9. A. Deltuva (2015), "Faddeev-type calculation of (d, n) transfer reactions in three-body nuclear systems", *Phys. Rev. C* 92, 064613.
10. A. Deltuva, A. C. Fonseca (2015), "Four-body calculation of elastic deuteron-deuteron scattering", *Phys. Rev. C* 92, 024001 (2015).
11. N. J. Upadhyay, A. Deltuva, F. M. Nunes (2012), "Testing the continuum-discretized coupled channels method for deuteron-induced reactions", *Phys. Rev. C* 85, 054621.
12. A. M. Mukhamedzhanov, V. Eremenko and A. I. Sattarov (2012), "Generalized Faddeev equations in the Alt-Grassberger-Sandhas form for deuteron stripping with explicit inclusion of target excitations and Coulomb interaction", *Phys. Rev. C* 86, 034001.
13. E. O. Alt, W. Sandhas, and H. Ziegelmann (1985), "Calculation of Proton-Deuteron Phase Parameters Including the Coulomb Force", *Nucl. Phys. A* 445, 429.

14. E. O. Alt, A. M. Mukhamedzhanov, A. I. Sattarov (1998), "Calculation of Proton-Deuteron Elastic Scattering at 10 MeV with a Realistic Potential", *Phys. Rev. Lett.* 81, 4820.
15. E. O. Alt, A. M. Mukhamedzhanov, M. M. Nishonov, and A. I. Sattarov (2002), "Proton-deuteron elastic scattering from 2.5 to 22.7 MeV", *Phys. Rev. C* 65, 064613.
16. E. O. Alt, A. S. Kadyrov, and A. M. Mukhamedzhanov (1996), "Approximate triangle amplitude for three-body charge exchange processes", *Phys. Rev. A* 53, 2438.
17. E. I. Dolinskii and A. M. Mukhamedzhanov (1966), "Coulomb effect in Direct Nuclear Reactions", *Soviet Journal of Nuclear Physics* 3, pp 180.
18. S. Okubo and D. Feldman (1960), "Some Aspects of the Covariant Two-Body Problem. I. The Bound-State Problem", *Phys. Rev.* 117, pp 292.
19. J. Schwinger (1964), "Coulomb Green's Function", *J. Math. Phys.* 5, pp 1606.
20. A. M. Mukhamedzhanov (1982), "Three-body Coulomb Green Function and the reactions with charged particles at low energies", *Czech. J. Phys. B* 32, pp 298.
21. L. D. Blokhintsev, A. M. Mukhamedzhanov and A. N. Safronov (1984), "Coulomb effects in nuclear reactions with charged particles", *Sov. J. Part. Nucl.* 15, pp 580.
22. G. V. Avakov, L. D. Blokhintsev, A. M. Mukhamedzhanov and R. Yarmukhamedov (1986), "Three-Particle Coulomb Effects in Nuclear Reactions with Three Charged Particles", *Sov. J. Nucl. Phys.* 43, pp 524.